

Surprisingly Good Performance of XYG3 Family Functionals Using Scaled KS-MP3 Correlation

*Golokesh Santra, Emmanouil Semidalas, and Jan M.L. Martin**

Department of Molecular Chemistry and Materials Science, Weizmann Institute of Science, 7610001 Rehovot, Israel.

Email: gershom@weizmann.ac.il

Abstract: By adding a GLPT3 (third-order Görling-Levy perturbation theory, or KS-MP3) term E_3 to the XYG7 form for a double hybrid, we are able to bring down WTMAD2 (weighted total mean absolute deviation) for the very large and chemically diverse GMTKN55 benchmark to an unprecedented 1.17 kcal/mol, competitive with much costlier composite wavefunction ab initio approaches. Intriguingly: (a) the introduction of E_3 makes an empirical dispersion correction redundant; (b) GGA or mGGA semilocal correlation functionals offer no advantage over LDA in this framework; (c) if a dispersion correction is retained, then simple Slater exchange leads to no significant loss in accuracy. It is possible to create a 6-parameter functional with WTMAD2=1.42 that has no post-LDA DFT components and no dispersion correction in the final energy.

Over the past few decades, Kohn-Sham density functional theory¹ (KS-DFT) has become the *go-to* electronic structure method, especially for medium and large molecular systems, as it combines reasonable accuracy with relatively mild computational cost-scaling with system size.² Being at the top of the ‘*Jacob’s Ladder*’ of density functional approximations,³ double hybrid density functionals (DHs) (see Refs.^{4–8} for reviews) are the most accurate DFT methods available to date for modeling a variety of chemical problems, like main group energetics,^{9–11} transition metal catalysis,^{12–15} electronic excitation spectroscopy,^{16–24} external magnetic^{25–28} and electric field^{29,30} response properties, and so on. Double hybrids can be further categorized according to their use of lower rung (hybrid) functionals in the orbital generation step as gDHs (after Grimme³¹) and xDHs (after the XYG3³² and related functionals⁵). Xu and co-workers used B3LYP^{33–35} orbitals while calculating the final energy for the original XYG3³² functional and its later variants, Irc-XYG3³⁶ and XYGJ-OS.³⁷ Along this line, xDSD,^{38–40} ω DSD,³⁹ and ω DSD3⁴¹ functionals from Martin group and the combinatorially optimized range separated double hybrid, ω B97M(2)⁴² by Mardirossian and Head-Gordon have shown remarkable performance for extensive and chemically diverse main-group benchmark like MGCDDB84⁹ (Main-Group Chemistry Database with about 5000 test cases divided into 84 subsets) and GMTKN55¹⁰ (General Main-group Thermochemistry, Kinetics, and Noncovalent interactions, 55 problem subsets). In a recent study, Zhang and Xu⁴³ explored the limits of the XYG3-type double hybrids utilizing B3LYP reference orbitals to be consistent with the original XYG3 functional. By gradually relaxing the constraints of the XYG3 they were able to improve the performance of their new xDHs and with all the constraints removed, XYG7@B3LYP appeared as the best in class. Their most intriguing finding was that decoupling Slater exchange from the GGA enhancement factor, i.e., giving B88x and pure Slater exchange independent coefficients, markedly improved performance.

In this letter, we consider two avenues for potential further improvement over XYG7@B3LYP. First, whether there might be more suitable orbitals than B3LYP for this type of functionals. Second, in light of our previous findings for the DSD3 and ω DSD3 functionals,⁴¹

whether it would be advantageous to add a scaled nonlocal GLPT3 (third-order Görling-Levy⁴⁴ perturbation theory) term on top of the same-spin and opposite-spin GLPT2 (second-order GLPT) terms already present. To answer both questions, we begin by employing reference orbitals where the percentage HF-like exchange (HFx) is increased systematically. Following Ref. ⁴³, the number m in XYG m refers to the number of terms considered; as we shall add a D3BJ^{45–47} empirical dispersion correction term, we shall refer to these xDH's as XYG8@BnLYP and XYG9@BnLYP, where n stands for the percentage of HFx used in the orbital generation. The final energy expressions of the XYG8@BnLYP and XYG9@BnLYP functionals have the form:

$$E_{\text{XYG8@BnLYP}} = E_{\text{N1e}} + c_{\text{X,HF}}E_{\text{X,HF}} + c_{\text{X,GGA}}E_{\text{X,B88}} + c_{\text{X,LDA}}E_{\text{X,Slater}} + c_{\text{C,GGA}}E_{\text{C,LYP}} \\ + c_{\text{C,LDA}}E_{\text{C,VWN5}} + c_{2\text{ab}}E_{2\text{ab}} + c_{2\text{ss}}E_{2\text{ss}} + s_6E_{\text{disp}}$$

$$E_{\text{XYG9@BnLYP}} = E_{\text{N1e}} + c_{\text{X,HF}}E_{\text{X,HF}} + c_{\text{X,GGA}}E_{\text{X,B88}} + c_{\text{X,LDA}}E_{\text{X,Slater}} + c_{\text{C,GGA}}E_{\text{C,LYP}} \\ + c_{\text{C,LDA}}E_{\text{C,VWN5}} + c_{2\text{ab}}E_{2\text{ab}} + c_{2\text{ss}}E_{2\text{ss}} + c_3E_3 + s_6E_{\text{disp}}$$

In both expressions, E_{N1e} stands for the sum of nuclear repulsion and one-electron energy terms; $E_{\text{X,HF}}$ represents the Hartree–Fock (HF) like exact exchange and $c_{\text{X,HF}}$ the corresponding coefficient; $E_{\text{X,B88}}$ and $E_{\text{X,Slater}}$ are the exchange energy components from the semilocal Becke88 generalized gradient approximation (GGA) and Slater-type local density approximation (LDA) — $c_{\text{X,GGA}}$ and $c_{\text{X,LDA}}$ are corresponding parameters respectively. The semilocal GGA and LDA correlation energies are represented by $E_{\text{C,LYP}}$ and $E_{\text{C,VWN5}}$, where $c_{\text{C,GGA}}$ and $c_{\text{C,LDA}}$ are the respective coefficients for those energy components. $E_{2\text{ab}}$ and $E_{2\text{ss}}$ are the opposite-spin and same-spin GLPT2 energies, E_3 is the GLPT3 energy, and $c_{2\text{ab}}$, $c_{2\text{ss}}$, and (for XYG9) c_3 are their respective linear coefficients. Finally, E_{disp} is a dispersion correction such as D3(BJ)^{45–47} or D4^{48–50}, each coming with adjustable parameters. In the present work, the dispersion energy term is made proportional to a linear coefficient s_6 .

In the discussion below, XYG8[f1]@BnLYP will indicate that one parameter was frozen, XYG8[f2]@BnLYP that two parameters were frozen, and so on.

Unlike B3LYP, BnLYP reference orbitals used for our XYG8 and XYG9 functionals do not contain any “unenhanced” Slater exchange. The BnLYP orbitals only differ in the exchange part where $n\%$ HFx and $(100-n)\%$ DFTx are used while the correlation part is kept unchanged throughout (19% VWN5 + 81% LYP). During the orbital generation and the final energy evaluation step, we make use of the same semilocal GGA-type and LDA-type exchange and correlation functionals.

For the present study, we have used the aforementioned GMTKN55 benchmark suite¹⁰ throughout to validate and parametrize our new functionals. It comprises 55 types of chemical problems, which can be further classified into five major subcategories: thermochemistry of small and medium-sized molecules, barrier heights, large-molecule reactions, intermolecular interactions, and conformer energies (or intramolecular interactions) (for the details of all 55 subsets with proper references see Table S1 in Supporting Information). The WTMAD2 (so-called weighted total mean absolute deviation of type 2) has been used as our primary metric of choice:

$$\text{WTMAD2} = \frac{1}{\sum_{i=1}^{55} N_i} \cdot \sum_{i=1}^{55} N_i \cdot \frac{56.84 \text{ kcal/mol}}{|\Delta E|_i} \cdot \text{MAD}_i$$

where $\overline{|\Delta E|}_i$ is the mean absolute value of all the reference energies from $i = 1$ to 55, N_i is the number of systems in each subset, MAD_i is the mean absolute difference between calculated and reference energies for each of the 55 subsets.

All electronic structure calculations except the third-order Møller-Plesset correlation (MP3) part were performed using the MRCC2020⁵¹ package. The Weigend–Ahlich family def2-QZVPP⁵² basis set was used for all subsets except for the anion-containing ones WATER27, RG18, IL16, G21EA, BH76, BH76RC and AHB21 – where the diffuse-function augmented def2-QZVPPD⁵³ was employed instead – and the C60ISO and UPU23 subsets, where we settled for the def2-TZVPP basis set to reduce computational cost. To reduce the latter further, the corresponding standard RI⁵⁴ and RI-JK⁵⁵ basis sets were employed for the correlation as well as for the Coulomb (J) and HF exchange (K) parts. The LD0110-LD0590 angular integration grid was used throughout, being a pruned Lebedev-type integration grid similar to Grid=UltraFine in Gaussian⁵⁶ or SG-3 in Q-Chem.⁵⁷ The same frozen core settings were used as in Refs.^{40,41} MP3 calculations in both HF and KS orbitals were performed using Q-Chem 5.4,⁵⁷ def2-TZVPP being used throughout – we previously found that this basis set is adequate for post-MP2 corrections, both in composite WFT and in double-hybrid DFT contexts.^{41,58} All calculations were performed on the ChemFarm HPC cluster in the Faculty of Chemistry at the Weizmann Institute of Science.

A fully optimized XYG8@BnLYP functional has eight adjustable parameters: $C_{X,HF}$, $C_{X,GGA}$, $C_{X,LDA}$, $C_{C,GGA}$, $C_{C,LDA}$, C_{2ab} , $C_{2ss}(=C_{2aa}+C_{2bb})$, and for the D3(BJ) dispersion correction, one prefactor s_6 and one parameter a_2 for the damping function (like in refs^{59,60} we constrain $a_1=s_8=0$). The XYG9@BnLYP functional has one additional prefactor (c_3) for the E_3 component.

We employed Powell’s BOBYQA⁶¹ (Bound Optimization BY Quadratic Approximation) derivative-free constrained optimizer, together with scripts and Fortran programs developed in-house, for the optimization of all parameters.

The statistical significance of adding or omitting a parameter was decided with the help of the Bayesian Information Criterion.^{62,63} For the dataset at hand (see Appendix A in the Supporting Information for details), a change of ~0.6% in WTMAD2 corresponds to “strong” and ~3.5% to “decisive” importance according to the Kass-Raftery criteria.⁶³

We first explore the performance of the XYG8@BnLYP functionals with n ranging from 10-70%. The minimum WTMAD2 occurs near $n = 20\%$; in fact, the WTMAD2 surface is relatively flat between 20-30%. While optimizing all eight parameters, the coefficient for the semilocal GGA-type correlation ($C_{C,GGA}$) settles near *zero*, thus fixing it to zero and reoptimizing the remaining seven parameters led us to WTMAD2=1.85 kcal/mol. That being said, the XYG8[f1]@B₂₅LYP and XYG8[f1]@B₃₀LYP are two very close contenders – which illustrates the flat behavior of the WTMAD2 surface between the 20-30% region (see Figure1).

Next, what if we leave out the dispersion component entirely, thus eliminating one additional parameter? On average, this would sacrifice only ~0.08 kcal/mol accuracy in terms of total WTMAD2, or about 4% of the total, which just exceed the “decisive” BIC criterion. As expected, among the top five subcategories of GMTKN55, the noncovalent interactions, and to some extent, barrier heights are most affected (see Table S2 in the Supporting Information). Although the D3BJ-uncorrected XYG8[f2]@B₂₅LYP functional offers the lowest WTMAD2 (1.92 kcal/mol), the performances of the XYG8[f2] variants utilizing B₂₀LYP and B₃₀LYP orbitals are pretty close.

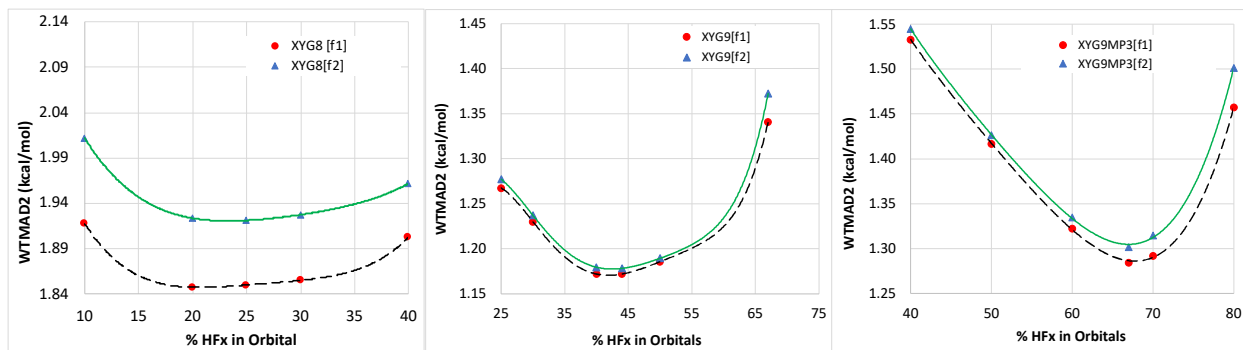


Figure 1: Effect of different orbitals on the total WTMAD2 (kcal/mol) for the PT2-based (left), KS-MP3 based (center) and canonical MP3 based (right) xDHs.

For the XYG8[f1]@BnLYP functionals, the coefficients for the GGA exchange (i.e., $c_{X,GGA}$) decrease as n increases (see Table 1). So, together with $c_{C,GGA}$ if we also fix $c_{X,GGA}$ at zero and optimize the remaining coefficients, the WTMAD2 difference between the XYG8[f1]@BnLYP and the new form, XYG8[f2g]@BnLYP, becomes narrower with increasing HF-like exchange in the orbitals and almost invisible for $n = 70\%$ (see Table 1). The letter g in XYG8[f2g]@BnLYP refers to the nature of the frozen parameters — g for GGA and l for LDA. Going from XYG8[f1]@B₂₀LYP to XYG8[f2g]@B₂₀LYP WTMAD2 increases by 0.16 kcal/mol. Now, comparing these two for the five top-level subsets, performance for all four top-level subsets other than barrier heights is degraded by imposing the $c_{X,GGA}=c_{C,GGA}=0$ constraint (see Table S2). Interestingly, among the small molecule thermochemistry subsets, the G21EA subset actually improves by imposing that constraint. Now, if we omit the dispersion correction term only and reoptimize everything else (i.e., XYG8[f1d]@B₂₀LYP, where d stands for dispersion), we obtain WTMAD2= 1.92 kcal/mol, which is practically the same as what we got for the XYG8[f2]@B₂₀LYP functional. Interestingly for XYG8[f1]@B₂₀LYP, if both s_6 and $c_{X,GGA}$ are frozen (i.e., XYG8[f3]) this drives up WTMAD2 by almost 1 kcal/mol, an order of magnitude more than freezing each of these individually (see Table S1 in the Supporting Information).

Next, as a control experiment: by fixing the coefficients for the LDA exchange and correlation ($c_{C,LDA}$ and $c_{X,LDA}$) at zero, we always obtain higher WTMAD2 than the corresponding functional forms where both $c_{X,GGA}$ and $c_{C,GGA}$ are zero. Once again, the WTMAD2 difference seems to become narrower for larger values of n (see Table S2 in the Supporting Information). The best pick in this category, the XYG8[f2l]@B₅₀LYP offers WTMAD2= 2.12 kcal/mol, which is comparable to our group's latest xDHs, xDSD₇₅-PBEP86-D3BJ (WTMAD2 = 2.14 kcal/mol) and xDSD₇₅-PBEP86-D4 (WTMAD2 = 2.12 kcal/mol).³⁹ Incidentally, for XYG8[f5]@B₂₀LYP, using only 100% HF-like exchange with scaled LDAc and PT2 correlation, WTMAD2 rises to 3.59 kcal/mol (see Table 1).

We now explore the effect of using different LDA semilocal correlations for the construction of these new functionals. XYG7@B3LYP is chosen for this purpose, where the VWN3 correlation is replaced by VWN5. For B3LYP orbitals, we also checked PW92 and found the results to be essentially the same as for VWN5 (see Table S3 and S4 in the Supporting Information). Without further optimization, the original XYG7⁴³ offers WTMAD2=1.88 kcal/mol, which is 0.17 kcal/mol lower than the value reported by Zhang and Xu. This discrepancy could be attributed to differences in the basis sets used, particularly for anionic subsets.

Table 1: Total WTMA22 (kcal/mol) and final parameters for the PT2-based XYG8@BnLYP double hybrids.^[a]

Functionals	Parameters								WTMA22 (kcal/mol)
	C _{X,HF}	C _{X,GGA}	C _{X,LDA}	C _{C,GGA}	C _{C,LDA}	C _{2ab}	C _{2ss}	S ₆ ^[b]	
XYG8[f1]@B ₁₀ LYP	0.8226	-0.0929	0.2530	[0]	0.5627	0.3407	0.1989	0.2457	1.918
XYG8[f2]@B ₁₀ LYP	0.8921	-0.1687	0.2447	[0]	0.5937	0.3488	0.2824	[0]	2.012
XYG8[f2g]@B ₁₀ LYP	0.7570	[0]	0.2421	[0]	0.5480	0.3133	0.1743	0.4399	2.052
XYG8[f2l]@B ₁₀ LYP	0.8382	0.1539	[0]	0.6991	[0]	0.3185	0.2701	0.2386	2.254
XYG8[f1]@B₂₀LYP	0.8482	-0.0935	0.2270	[0]	0.5243	0.3985	0.2162	0.2060	1.848
XYG8[f2]@B₂₀LYP	0.9085	-0.1603	0.2236	[0]	0.5264	0.4189	0.2780	[0]	1.924
XYG8[f2g]@B ₂₀ LYP	0.7807	[0]	0.2117	[0]	0.5436	0.3567	0.1996	0.4206	2.003
XYG8[f2l]@B ₂₀ LYP	0.8576	0.1373	[0]	0.6249	[0]	0.3864	0.2773	0.2072	2.179
XYG8[f5]@B ₂₀ LYP	[1.0]	[0]	[0]	[0]	0.6113	0.3835	0.6174	[0]	3.594
XYG8[f1]@B ₂₅ LYP	0.8724	-0.1071	0.2097	[0]	0.5299	0.4233	0.2468	0.1550	1.850
XYG8[f2]@B ₂₅ LYP	0.9144	-0.1537	0.2132	[0]	0.4928	0.4540	0.2780	[0]	1.921
XYG8[f2g]@B ₂₅ LYP	0.7921	[0]	0.2033	[0]	0.5026	0.3978	0.1987	0.3952	1.991
XYG8[f2l]@B ₂₅ LYP	0.8638	0.1334	[0]	0.5803	[0]	0.4202	0.2884	0.2006	2.161
XYG8[f1]@B ₃₀ LYP	0.8674	-0.0922	0.2015	[0]	0.5096	0.4501	0.2397	0.1824	1.855
XYG8[f2]@B ₃₀ LYP	0.9180	-0.1458	0.1986	[0]	0.4964	0.4728	0.2949	[0]	1.928
XYG8[f2g]@B ₃₀ LYP	0.7972	[0]	0.1953	[0]	0.4992	0.4188	0.2076	0.3846	1.987
XYG8[f2l]@B ₃₀ LYP	0.8577	0.1409	[0]	0.5530	[0]	0.4485	0.2777	0.2351	2.146
XYG8[f1]@B ₄₀ LYP	0.8951	-0.1015	0.1754	[0]	0.5075	0.5004	0.2896	0.1169	1.903
XYG8[f2]@B ₄₀ LYP	0.9229	-0.1334	0.1762	[0]	0.4982	0.5132	0.3244	[0]	1.962
XYG8[f2g]@B ₄₀ LYP	0.8090	[0]	0.1855	[0]	0.4378	0.4902	0.2034	0.3589	1.987
XYG8[f2l]@B ₄₀ LYP	0.8555	0.1421	[0]	0.5139	[0]	0.5012	0.2797	0.2506	2.129
XYG8[f1]@B ₅₀ LYP	0.8712	-0.0702	0.1738	[0]	0.4555	0.5519	0.2595	0.1856	1.935
XYG8[f2]@B ₅₀ LYP	0.9269	-0.1227	0.1608	[0]	0.4661	0.5779	0.3326	[0]	2.005
XYG8[f2g]@B ₅₀ LYP	0.8199	[0]	0.1681	[0]	0.4344	0.5296	0.2457	0.3315	1.988
XYG8[f2l]@B ₅₀ LYP	0.8543	0.1401	[0]	0.4951	[0]	0.5555	0.2756	0.2535	2.119
XYG8[f1]@B ₆₀ LYP	0.8753	-0.0684	0.1632	[0]	0.4411	0.5933	0.2931	0.1696	1.997
XYG8[f2]@B ₆₀ LYP	0.9197	-0.1156	0.1593	[0]	0.4281	0.6269	0.3417	[0]	2.080
XYG8[f2g]@B ₆₀ LYP	0.8146	[0]	0.1726	[0]	0.4022	0.5861	0.2245	0.3328	2.006
XYG8[f2l]@B ₆₀ LYP	0.8623	0.1277	[0]	0.4655	[0]	0.6096	0.3062	0.2110	2.129
XYG8[f1]@B ₇₀ LYP	0.8413	-0.0318	0.1631	[0]	0.4294	0.6213	0.2803	0.2548	2.106
XYG8[f2]@B ₇₀ LYP	0.9167	-0.1014	0.1442	[0]	0.4488	0.6572	0.3803	[0]	2.227
XYG8[f2g]@B ₇₀ LYP	0.8142	[0]	0.1682	[0]	0.4026	0.6250	0.2431	0.3227	2.108
XYG8[f2l]@B ₇₀ LYP	0.8222	0.1675	[0]	0.4796	[0]	0.6258	0.2821	0.3118	2.200

^[a]parameters in square bracket are the constraints we used. ^[b]a₂ is kept constant at 5.6 throughout.

In 2003, Grimme introduced the SCS-MP3 method, which outperformed regular MP3 at no extra cost;⁶⁴ later, Hobza and coworkers⁶⁵ coined the term MP2.5 for the average of MP2 and MP3, and showed its superior performance for noncovalent interactions. Recently, we have reported⁴¹ that adding an MP3-like correlation term in the final KS energy expression can significantly improve the performances of both global and range-separated DSD double hybrids, albeit at some extra computational expense. As technical limitations precluded using KS reference orbitals for MP3 at that time, we used the HF reference orbitals to calculate the conventional MP3 correlation energies and added them into the DSD and ω DSD functional forms with an additional linear coefficient. Motivated by the above two findings, here we combine the scaled E_3 correlation energies with the XYG8@BnLYP functionals to check whether it is possible to improve their performance further. Similar to Ref.⁴¹, we have omitted the 50 largest systems, i.e., the UPU23 and C60 subsets, ten largest ISOL24, three INV24, and a single IDISP, we refer to this reduced version of GMTKN55 as mod-GMTKN55 in this paper.

Surprisingly enough, the lowest WTMAD2 we got is 1.28 kcal/mol using the B₆₇LYP orbitals. Similar to the PT2 based functionals above, here too, the optimized C_{C,GGA} values approach zero, and thus C_{C,GGA} can be eliminated without any accuracy loss (see Table 2). Upon comparing the performance of the eight parameter XYG9_{MP3}[f1]@B₆₇LYP with the PT2 based XYG8[f1]@B₂₀LYP for the five top-level subsets, we find that the lion’s share of the WTMAD2 improvement is seen in the small and medium molecule thermochemistry and large molecule reactions subsets. Next, comparing the XYG9_{MP3}[f1] with the PT2-based XYG8[f1] evaluated using the same set of orbitals, namely B₆₇LYP, we find that statistics of large-molecule reactions subset improve by 50% upon inclusion of MP3 correlation (see Table S5 in the Supporting Information).

Table 2: Total WTMAD2 (kcal/mol) and final parameters for the XYG9_{MP3}@B_nLYP double hybrids.^[a]

Functionals	Parameters									WTMAD2 (kcal/mol)
	C _{X,HF}	C _{X,GGA}	C _{X,LDA}	C _{C,GGA}	C _{C,LDA}	C _{2ab}	C _{2aa}	C ₃	S ₆ ^[b]	
XYG9 _{MP3} [f1]@B ₁₀ LYP	0.8784	-0.1297	0.2341	[0]	0.5176	0.3704	0.2917	0.1574	0.1349	1.783
XYG9 _{MP3} [f2]@B ₁₀ LYP	0.9180	-0.1675	0.2237	[0]	0.5433	0.3742	0.3465	0.1702	[0]	1.838
XYG9 _{MP3} [f1]@B ₂₀ LYP	0.8862	-0.1073	0.2060	[0]	0.4718	0.4306	0.3002	0.1591	0.1548	1.671
XYG9 _{MP3} [f2]@B ₂₀ LYP	0.9392	-0.1499	0.1880	[0]	0.4733	0.4449	0.3872	0.2120	[0]	1.694
XYG9 _{MP3} [f1]@B ₂₅ LYP	0.9309	-0.1197	0.1722	[0]	0.4356	0.4758	0.3894	0.2290	0.0612	1.641
XYG9 _{MP3} [f2]@B ₂₅ LYP	0.9454	-0.1405	0.1757	[0]	0.4320	0.4851	0.3936	0.2178	[0]	1.659
XYG9 _{MP3} [f1]@B ₃₀ LYP	0.9395	-0.1080	0.1504	[0]	0.4220	0.5033	0.4322	0.2624	0.0617	1.609
XYG9 _{MP3} [f2]@B ₃₀ LYP	0.9538	-0.1318	0.1542	[0]	0.4367	0.5037	0.4437	0.2595	[0]	1.625
XYG9 _{MP3} [f1]@B ₄₀ LYP	0.9387	-0.0875	0.1324	[0]	0.3744	0.5726	0.4398	0.2667	0.0851	1.533
XYG9 _{MP3} [f2]@B ₄₀ LYP	0.9617	-0.1087	0.1299	[0]	0.3530	0.5914	0.4695	0.2845	[0]	1.545
XYG9 _{MP3} [f1]@B ₅₀ LYP	0.9627	-0.0659	0.0901	[0]	0.2888	0.6657	0.5718	0.4224	0.0568	1.417
XYG9 _{MP3} [f2]@B ₅₀ LYP	0.9786	-0.0831	0.0918	[0]	0.2684	0.6867	0.5638	0.3986	[0]	1.426
XYG9 _{MP3} [f1]@B ₆₀ LYP	0.9582	-0.0500	0.0794	[0]	0.2395	0.7424	0.6019	0.4554	0.0649	1.322
XYG9 _{MP3} [f2]@B ₆₀ LYP	0.9789	-0.0625	0.0680	[0]	0.2492	0.7512	0.6419	0.4653	[0]	1.335
XYG9_{MP3}[f1]@B₆₇LYP	0.9490	-0.0182	0.0606	[0]	0.1907	0.8002	0.6676	0.5381	0.0962	1.284
XYG9_{MP3}[f2]@B₆₇LYP	0.9807	-0.0408	0.0478	[0]	0.1935	0.8165	0.7218	0.5557	[0]	1.301
XYG9 _{MP3} [f2g]@B ₆₇ LYP	0.9391	[0]	0.0548	[0]	0.1927	0.7902	0.6818	0.5491	0.1269	1.297
XYG9 _{MP3} [f3]@B ₆₇ LYP	0.9834	[0]	0.0121	[0]	0.1572	0.8291	0.8320	0.6478	[0]	1.378
XYG9 _{MP3} [f1]@B ₇₀ LYP	0.9360	-0.0029	0.0589	[0]	0.1880	0.8089	0.6796	0.5515	0.1269	1.292
XYG9 _{MP3} [f2]@B ₇₀ LYP	0.9778	-0.0367	0.0426	[0]	0.2161	0.8207	0.7527	0.5678	[0]	1.315
XYG9 _{MP3} [f1]@B ₈₀ LYP	0.9088	0.0241	0.0577	[0]	0.1830	0.8517	0.7173	0.5751	0.1606	1.457
XYG9 _{MP3} [f2]@B ₈₀ LYP	0.9673	-0.0157	0.0365	[0]	0.1376	0.9242	0.8108	0.6593	[0]	1.501

^[a]parameters in square brackets are the constraints we used. ^[b]a₂ is kept constant at 5.6 throughout.

In Ref.⁴¹, for none for the global or range-separated DSD3 functionals could we omit the dispersion correction term with impunity: for instance, ωDSD3-PBEP86-D3BJ offered WTMAD2 = 2.08 kcal/mol while the dispersion-free variant ωDSD3-PBEP86 has WTMAD2 = 2.86 kcal/mol (see Table 3 in Ref.⁴¹). However, for the present conventional-MP3-based XYG9_{MP3}[f1]@B_nLYP functionals, discarding the dispersion term has only a negligible effect on total WTMAD2 (~0.01-0.02 kcal/mol) — which is a much narrower range compared to that in PT2-based XYG8[f1]@B_nLYP functionals (see Figures 1).

We now examine the importance of considering the semilocal DFT exchange coefficient (C_{X,GGA}). The optimized C_{X,GGA} values decrease as *n* increases (see Table 2). If we fix both C_{X,GGA} and C_{C,GGA} at zero and optimize other coefficients (i.e., XYG9_{MP3}[f2g]@B₆₇LYP), the resulted WTMAD2 goes up only a negligible amount compared to that for the XYG9_{MP3}[f1]@B₆₇LYP. Now, if we also

discard the empirical dispersion correction term — which leaves us with only six adjustable parameters (same as our group's revDSD-PBEP86-D3BJ⁴⁰), we get WTMAD2 = 1.38 kcal/mol. So, for these PT3-containing double hybrids, the dispersion correction term is nearly redundant as far as total WTMAD2 is concerned.

Thus far, we have used canonical MP3 correlation energies as an additional component to improve the performance of GLPT2 based XYG8[f1]@BnLYP double hybrids. In a recent study, Head-Gordon and co-workers have shown^{66,67} that the use of DFT orbitals instead of pure HF ones for MP3 calculation can significantly improve performance for thermochemistry, barrier heights, noncovalent interactions, and dipole moments. Additionally, Jana et al.⁶⁸ have found that considering Görling–Levy perturbation terms beyond second order can improve the performance of PBE-based double hybrids for some selected datasets. So, here we explore whether employing the scaled MP3 correlation energies evaluated *in a basis of BnLYP orbitals (i.e., KS-MP3)* can still be beneficial compared to the already excellent XYG9_{MP3}@BnLYP functionals. We have used the same mod-GMKN55 dataset for the parametrization as well as validation of these functionals.

We again notice that $c_{C,GGA}$ settles near zero after optimization, so we proceed by setting it to *zero* and refitting the eight remaining parameters for the KS-MP3 based functionals (namely XYG9[f1]@BnLYP). Using 44% HFx in the orbital generation step, the XYG9[f1]@B₄₄LYP offers the lowest WTMAD2 (1.17 kcal/mol), which is even lower than what we got for the top canonical MP3 based xDH, XYG9_{MP3}[f1]@B₆₇LYP(1.28 kcal/mol). However, the WTMAD2 surface for XYG9[f1]@BnLYP is pretty flat between the 40-50% region (see Figure 1). That being said, the performance of the XYG9[f1]@B₄₄LYP is now in the territory of the best G4-type composite WFT methods (cWFT), recently proposed by Semidalas and Martin.^{58,69} It actually surpasses the performance of the G4-T approach⁵⁸ by 0.34 kcal/mol; the improvement lies mainly in conformers and to a lesser degree in large molecule energetics (see Table 1 in Ref.⁵⁸). The correlation consistent cc-G4-type protocols⁶⁹ still have an edge over XYG9[f1]@B₄₄LYP, but the accuracy gap has narrowed even more since the top cWFT performers, cc-G4-T and the parameter-free cc-G4-F12-T, have WTMAD2 = 0.90 and 1.04 kcal/mol, respectively.

Now, comparing the XYG9[f1]@B₄₄LYP with the PT2-based XYG8[f1]@B₂₀LYP (WTMAD2 = 1.79 kcal/mol for mod-GMKN55) for the five top-level subsets, we found that the large molecule reactions and small molecule thermochemistry are the two most benefited classes. Let's check where exactly KS-MP3 based functionals benefit over the canonical MP3 based variants. We compare the WTMAD2 contribution of individual subsets between the XYG9[f1] and XYG9_{MP3}[f1] (WTMAD2=1.49 kcal/mol) functionals evaluated over the same set of KS orbitals, B₄₄LYP (see Table S12 and S17 in the Supporting Information). Although performance improved for most of the subsets, the top affected subsets are: TAUT15, RSE43, HAL59, PAREL, MCONF, G21EA and CDIE20.

Now, what if we leave the dispersion correction out entirely? The WTMAD2 gap between the XYG9[f1]@BnLYP and XYG9[f2]@BnLYP then almost vanishes (see Figure 1). Due to the negligible effect of the dispersion correction term, we elected not to fit the more advanced D4^{49,50} dispersion correction on top of XYG9[f2]@BnLYP. At a reviewer's request, a plot of the interaction energy of stretched Ar₂ can be found in the Supporting Information (see Figure S2): proper asymptotic R⁻⁶ dependence is observed there, indicating this was not sacrificed by omitting the dispersion correction.

Similar to the PT2 based XYG8@BnLYP and canonical MP3 based XYG9_{MP3}@BnLYP double hybrids, $c_{X,GGA}$ gradually decreases with the increase of n (see Table 3). Now, if we fix both $c_{X,GGA}$ and $c_{C,GGA}$ at zero and reoptimize the remain seven parameters, we obtain WTMAD2 = 1.25 kcal/mol. Additionally, if we also discard the empirical dispersion term (WTMAD2 = 1.42 kcal/mol), we lose a nontrivial amount (0.25 kcal/mol) of accuracy compared to our best pick XYG9[f1]@B₄₄LYP. In contrast, the loss in WTMAD2 is 0.17 kcal/mol compared to the corresponding D3BJ-uncorrected variant XYG9[f2]@B₄₄LYP.

Next, if we consider only pure HF-exchange (i.e., fixing $c_{X,HF}=1$) and optimize the four remaining correlation prefactors, we get WTMAD2 = 1.56 kcal/mol for the XYG9[f5]@B₄₄LYP (see Table 3). Comparing XYG9[f5]@B₄₄LYP with XYG9[f2]@BnLYP for all 55 subsets of GMTKN55, we find the greatest differences for BUT14DIOL, G21EA, RG18, and BSR36. However, we must mention that the resulting functional XYG9[f5]@B₄₄LYP is no longer a “double hybrid” in the usual sense, as we are mixing the semilocal and nonlocal terms only for the correlation part. However, if we additionally constrain $c_{C,LDA}=0$ for XYG9[f5]@B₄₄LYP (ak.a, XYG9[f6]@B₄₄LYP), WTMAD2 increases to 2.50 kcal/mol.

Table 3: Total WTMAD2 (kcal/mol) and final parameters for the KS-MP3 based XYG9@BnLYP double hybrids.^[a]

Functionals	Parameters									WTMAD2 (kcal/mol)
	$c_{X,HF}$	$c_{X,GGA}$	$c_{X,LDA}$	$c_{C,GGA}$	$c_{C,LDA}$	c_{2ab}	c_{2ss}	c_3	$s_6^{[b]}$	
XYG9[f1]@B ₁₀ LYP	0.9004	-0.1126	0.2028	[0]	0.4798	0.3751	0.4227	0.0918	0.0571	1.578
XYG9[f2]@B ₁₀ LYP	0.9154	-0.1319	0.2045	[0]	0.4763	0.3831	0.4361	0.0941	[0]	1.602
XYG9[f1]@B ₂₀ LYP	0.9276	-0.1025	0.1662	[0]	0.4179	0.4532	0.4760	0.1339	0.0408	1.302
XYG9[f2]@B ₂₀ LYP	0.9396	-0.1116	0.1619	[0]	0.4180	0.4558	0.5010	0.1389	[0]	1.316
XYG9[f1]@B ₂₅ LYP	0.9348	-0.0884	0.1450	[0]	0.3930	0.4868	0.5132	0.1588	0.0479	1.267
XYG9[f2]@B ₂₅ LYP	0.9440	-0.1020	0.1472	[0]	0.3982	0.4902	0.5192	0.1570	[0]	1.277
XYG9[f1]@B ₃₀ LYP	0.9358	-0.0793	0.1343	[0]	0.3749	0.5196	0.5186	0.1699	0.0580	1.230
XYG9[f2]@B ₃₀ LYP	0.9520	-0.0917	0.1302	[0]	0.3626	0.5305	0.5463	0.1791	[0]	1.237
XYG9[f1]@B ₄₀ LYP	0.9571	-0.0738	0.1098	[0]	0.2948	0.6157	0.5684	0.2249	0.0241	1.172
XYG9[f2]@B ₄₀ LYP	0.9602	-0.0804	0.1123	[0]	0.2974	0.6156	0.5640	0.2165	[0]	1.179
XYG9[f1]@B₄₄LYP	0.9508	-0.0502	0.0928	[0]	0.2880	0.6280	0.6144	0.2570	0.0579	1.172
XYG9[f2]@B₄₄LYP	0.9692	-0.0644	0.0881	[0]	0.2730	0.6447	0.6467	0.2761	[0]	1.178
XYG9[f2g]@B ₄₄ LYP	0.9165	[0]	0.0844	[0]	0.2836	0.6112	0.6048	0.2606	0.1687	1.252
XYG9[f3]@B ₄₄ LYP	0.9652	[0]	0.0430	[0]	0.2267	0.6564	0.7641	0.3303	[0]	1.424
XYG9[f5]@B ₄₄ LYP	[1.0]	[0]	[0]	[0]	0.2703	0.6535	0.8475	0.3488	[0]	1.557
XYG9[f6]@B ₄₄ LYP	[1.0]	[0]	[0]	[0]	[0]	0.6986	0.9857	0.4608	[0]	2.499
XYG9[f1]@B ₅₀ LYP	0.9654	-0.0529	0.0782	[0]	0.2631	0.6771	0.6675	0.3026	0.0173	1.186
XYG9[f2]@B ₅₀ LYP	0.9693	-0.0571	0.0785	[0]	0.2592	0.6809	0.6723	0.3047	[0]	1.189
XYG9[f1]@B ₆₇ LYP	0.9389	-0.0172	0.0674	[0]	0.2161	0.7795	0.6974	0.3912	0.0851	1.341
XYG9[f2]@B ₆₇ LYP	0.9667	-0.0403	0.0610	[0]	0.2113	0.8080	0.7144	0.3894	[0]	1.372

^[a]parameters in square brackets are the constraints we used. ^[b] a_2 is kept constant at 5.6 throughout.

For the XYG9[f1]@B₄₄LYP functionals, we note that the sum of three exchange parameters is very close to one. So, if we re-enforce the $c_{X,HF} + c_{X,GGA} + c_{X,LDA} = 1$ constraint (one among the four constraints of the original XYG3³²) and optimize the seven remaining parameters, how much performance is sacrificed? Performing this test on both the XYG9[f1]@B₄₀LYP and XYG9[f1]@B₄₄LYP and their D3BJ-uncorrected variants, we found that the loss in terms of WTMAD2 is almost imperceptible (see Table S3 in the Supporting Information). So, it is possible to reduce the number of parameters for both variants without sacrificing any significant accuracy.

A reviewer inquired about the counterintuitively negative $c_{X,GGA}$ coefficients in Table 3. In response, we carried out constrained reoptimizations for a sequence of fixed values of $c_{X,HF}$. The result can be found in the Supporting Information (see Figure S3). It can be seen there that $c_{X,GGA}$ has a linear dependence with a negative slope on $c_{X,HF}$; beyond ca. 87%, $c_{X,GGA}$ becomes negative. A tentative explanation can be advanced as follows: considering that $E_{X,B88}=E_{X,LDA}\cdot F_{B88}(s)$, where $F(s)$ is an enhancement factor depending on the reduced density gradient $s=\nabla\rho/\rho^{4/3}$, it follows that $c_{X,LDA}\cdot E_{X,LDA} + c_{X,GGA}\cdot E_{X,B88} = (c_{X,LDA}+c_{X,GGA})E_{X,LDA} + c_{X,GGA}(F_{B88}(s) - 1)$. Now as $F_{B88}(0)=1$ and $F(s)\geq 1$ for all s , a negative $c_{X,GGA}$ effectively implies that semilocal exchange will be progressively throttled as s becomes large (in the periphery of the atomic density), while a positive $c_{X,GGA}$ implies the opposite. It stands to reason that, as more “exact” exchange is introduced, the functional would increasingly benefit from semilocal exchange “getting out of the way” as s increases.

Lastly, by adding a KS-MP3 correlation component on top of XYG3@B3LYP and optimizing all four parameters against mod-GMTKN55, we get WTMAD2= 1.64 kcal/mol. On the other hand, doing the same for the XYG7@B3LYP offers WTMAD2= 1.35 kcal/mol (see Table S6 in the Supporting Information).

We can conclude the following from an extensive study of XYG8@BnLYP, XYG9_{MP3}@BnLYP and XYG9@BnLYP double-hybrid density functionals using the large and chemically diverse GMTKN55 and mod-GMTKN55 databases:

- For all three xDH variants we have discussed above, the optimized parameter for the semilocal DFT correlation is close to zero across the board and can be safely eliminated without sacrificing any accuracy in terms of WTMAD2.
- For the new PT2-based XYG8[f1]@BnLYP double hybrids, we found a minimum WTMAD2 when the final energies are evaluated over B₂₀LYP orbitals. However, the WTMAD2 surface is nearly flat over the 20-30% region.
- Including a scaled canonical MP3 term in the final energy significantly improves the performance, as previously found⁴¹ with the DSD3 and ω DSD3 functionals. The XYG9_{MP3}[f1]@B₆₇LYP now offers the lowest WTMAD2 (1.28 kcal/mol) among all the regular MP3 based XYG-type functionals tested above. Among the five top-level subsets, small-molecule thermochemistry and large molecule reactions are the two most benefited classes.
- Replacing the HF-based MP3 term by KS-MP3 further improved statistics, with XYG9[f1]@B₄₄LYP offering the lowest WTMAD2 (1.17 kcal/mol). To the authors’ knowledge, this is by far *the lowest reported WTMAD2 for any DFT method, and is in the same range as the G4-type composite WFT methods*. The WTMAD2 surface is almost flat around the minimum, in the n=40-50% region.
- Another advantage of adding a scaled E_3 correlation term in xDHs is that the dispersion correction becomes essentially redundant, unlike the case where E_3 is absent. As far as the D3BJ-uncorrected functionals are concerned, KS-MP3 based XYG9[f2]@B₄₄LYP is our best pick.
- Both for the PT2 based and MP3 based xDHs presented in this letter, the coefficient for the semilocal DFT exchange term decreases with increasing % HFx used during the orbital generation. Thus, this parameter can also be set to zero if one use orbitals with higher

fraction of HFx for the final energy evaluation. We note that this leads to a situation where the final energy expression is entirely independent of post-LDA enhancement factors in both exchange and correlation.

- Interestingly enough, using the full HF-like exchange and only the four correlation energy terms (i.e., $C_{C,LDA}$, C_{2ab} , C_{2SS} and c_3) in the final energy expression, we can achieve WTMAD2 = 1.56 kcal/mol for XYG9[f5]@B₄₄LYP, which is only 0.38 kcal/mol inferior to our best pick XYG9[f1]@B₄₄LYP.

A final remark is due on the computational cost. Table S18 and Figure S1 show wall clock time dependence on the system size in the ADIM6 subset (n-alkane dimers, n=2–7). XYG8[f1]@B₄₄LYP and other MP2-based double hybrids, in this size range and with the RI approximation, scale about $O(N^3)$ with basis set size. The RI-MP3 algorithm used scales almost like canonical $O(N^6)$, and hence that term rapidly dominates the overall calculation. However, recent developments^{67,70} in tensor hypercontraction approaches⁷¹ reduce scaling to $O(N^4)$ and may be effectively exploited here.

We would like to acknowledge helpful discussions with Prof. Dr. A. Daniel Boese (Karl-Franzens-Universität Graz, Austria). GS acknowledges a doctoral fellowship from the Feinberg Graduate School (WIS). The work of E.S. on this scientific paper was supported by the Onassis Foundation — Scholarship ID: F ZP 052-1/2019-2020. The authors would like to thank Dr. Nisha Mehta (WIS) for critical reading of the manuscript.

This research was funded by the Israel Science Foundation (grant 1969/20) and by the Minerva Foundation (grant 2020/05).

The Supporting Information (in PDF format) is available free of charge at

<https://doi.org/10.1021/xxxxxxx>.

Appendix on the Bayesian Information Criterion; Abridged details of all 55 subsets of GMTKN55 with proper references; Optimized parameters, total WTMAD2 and its division into five major subsets for several XYG8@B3LYP variants and original XYG7@B3LYP; Total WTMAD2 and its division into five major subsets for different variants of XYG8@B_nLYP, XYG9_{MP3}@B_nLYP and XYG9@B_nLYP; MAD, MSD and RMSD as well as breakdown of total WTMAD2 per subset for the XYG8[f1]@B₂₀LYP, XYG8[f2]@B₂₅LYP, original XYG7@B3LYP, XYG9_{MP3}[f1]@B₆₇LYP, XYG9_{MP3}[f1]@B₄₄LYP, XYG9_{MP3}[f2]@B₆₇LYP, XYG9[f1]@B₄₄LYP, XYG9[f2]@B₄₄LYP, XYG9[f2g]@B₄₄LYP, XYG9[f3]@B₄₄LYP, XYG9[f5]@B₄₄LYP ; and MRCC and QCHEM sample inputs for the XYG8[f1]@B₂₅LYP and XYG9[f2]@B₄₄LYP functionals.

- (1) Kohn, W.; Sham, L. J. Self-Consistent Equations Including Exchange and Correlation Effects. *Phys. Rev.* **1965**, *140* (4A), A1133–A1138. <https://doi.org/10.1103/PhysRev.140.A1133>.
- (2) Kohn, W.; Becke, A. D.; Parr, R. G. Density Functional Theory of Electronic Structure. *J. Phys. Chem.* **1996**, *100* (31), 12974–12980. <https://doi.org/10.1021/jp960669l>.

- (3) Perdew, J. P.; Schmidt, K. Jacob's Ladder of Density Functional Approximations for the Exchange-Correlation Energy. *AIP Conf. Proc.* **2001**, *577* (1), 1–20. <https://doi.org/10.1063/1.1390175>.
- (4) Goerigk, L.; Grimme, S. Double-Hybrid Density Functionals. *Wiley Interdiscip. Rev. Comput. Mol. Sci.* **2014**, *4* (6), 576–600. <https://doi.org/10.1002/wcms.1193>.
- (5) Zhang, I. Y.; Xu, X. Doubly Hybrid Density Functional for Accurate Description of Thermochemistry, Thermochemical Kinetics and Nonbonded Interactions. *Int. Rev. Phys. Chem.* **2011**, *30* (1), 115–160. <https://doi.org/10.1080/0144235X.2010.542618>.
- (6) Brémond, E.; Ciofini, I.; Sancho-García, J. C.; Adamo, C. Nonempirical Double-Hybrid Functionals: An Effective Tool for Chemists. *Acc. Chem. Res.* **2016**, *49* (8), 1503–1513. <https://doi.org/10.1021/acs.accounts.6b00232>.
- (7) Mehta, N.; Casanova-Páez, M.; Goerigk, L. Semi-Empirical or Non-Empirical Double-Hybrid Density Functionals: Which Are More Robust? *Phys. Chem. Chem. Phys.* **2018**, *20* (36), 23175–23194. <https://doi.org/10.1039/C8CP03852J>.
- (8) Martin, J. M. L.; Santra, G. Empirical Double-Hybrid Density Functional Theory: A 'Third Way' in Between WFT and DFT. *Isr. J. Chem.* **2020**, *60* (8–9), 787–804. <https://doi.org/10.1002/ijch.201900114>.
- (9) Mardirossian, N.; Head-Gordon, M. Thirty Years of Density Functional Theory in Computational Chemistry: An Overview and Extensive Assessment of 200 Density Functionals. *Mol. Phys.* **2017**, *115* (19), 2315–2372. <https://doi.org/10.1080/00268976.2017.1333644>.
- (10) Goerigk, L.; Hansen, A.; Bauer, C.; Ehrlich, S.; Najibi, A.; Grimme, S. A Look at the Density Functional Theory Zoo with the Advanced GMTKN55 Database for General Main Group Thermochemistry, Kinetics and Noncovalent Interactions. *Phys. Chem. Chem. Phys.* **2017**, *19* (48), 32184–32215. <https://doi.org/10.1039/C7CP04913G>.
- (11) Goerigk, L.; Mehta, N. A Trip to the Density Functional Theory Zoo: Warnings and Recommendations for the User. *Aust. J. Chem.* **2019**, *72* (8), 563–573. <https://doi.org/10.1071/CH19023>.
- (12) Dohm, S.; Hansen, A.; Steinmetz, M.; Grimme, S.; Checinski, M. P. Comprehensive Thermochemical Benchmark Set of Realistic Closed-Shell Metal Organic Reactions. *J. Chem. Theory Comput.* **2018**, *14* (5), 2596–2608. <https://doi.org/10.1021/acs.jctc.7b01183>.
- (13) Iron, M. A.; Janes, T. Correction to "Evaluating Transition Metal Barrier Heights with the Latest Density Functional Theory Exchange–Correlation Functionals: The MOBH35 Benchmark Database." *J. Phys. Chem. A* **2019**, *123* (29), 6379–6380. <https://doi.org/10.1021/acs.jpca.9b06135>.
- (14) Santra, G.; Martin, J. M. L. Some Observations on the Performance of the Most Recent Exchange-Correlation Functionals for the Large and Chemically Diverse GMTKN55 Benchmark. *AIP Conf. Proc.* **2019**, *2186*, 030004. <https://doi.org/10.1063/1.5137915>.
- (15) Efremenko, I.; Martin, J. M. L. Coupled Cluster Benchmark of New Density Functionals and Domain Pair Natural Orbital Methods: Mechanisms of Hydroarylation and Oxidative Coupling Catalyzed by Ru(II) Chloride Carbonyls. *AIP Conf. Proc.* **2019**, *2186*, 030005. <https://doi.org/10.1063/1.5137916>.
- (16) Grimme, S.; Neese, F. Double-Hybrid Density Functional Theory for Excited Electronic

- States of Molecules. *J. Chem. Phys.* **2007**, *127* (15), 154116.
<https://doi.org/10.1063/1.2772854>.
- (17) Goerigk, L.; Grimme, S. Calculation of Electronic Circular Dichroism Spectra with Time-Dependent Double-Hybrid Density Functional Theory. *J. Phys. Chem. A* **2009**, *113* (4), 767–776. <https://doi.org/10.1021/jp807366r>.
- (18) Goerigk, L.; Moellmann, J.; Grimme, S. Computation of Accurate Excitation Energies for Large Organic Molecules with Double-Hybrid Density Functionals. *Phys. Chem. Chem. Phys.* **2009**, *11* (22), 4611. <https://doi.org/10.1039/b902315a>.
- (19) Goerigk, L.; Kruse, H.; Grimme, S. Theoretical Electronic Circular Dichroism Spectroscopy of Large Organic and Supramolecular Systems. In *Comprehensive Chiroptical Spectroscopy*; Berova, N., Polavarapu, P. L., Nakanishi, K., Woody, R. W., Eds.; Wiley: Hoboken, NJ, USA, 2012; Vol. 1, pp 643–673.
<https://doi.org/10.1002/9781118120187.ch22>.
- (20) Schwabe, T.; Goerigk, L. Time-Dependent Double-Hybrid Density Functionals with Spin-Component and Spin-Opposite Scaling. *J. Chem. Theory Comput.* **2017**, *13* (9), 4307–4323. <https://doi.org/10.1021/acs.jctc.7b00386>.
- (21) Casanova-Páez, M.; Goerigk, L. Time-Dependent Long-Range-Corrected Double-Hybrid Density Functionals with Spin-Component and Spin-Opposite Scaling: A Comprehensive Analysis of Singlet–Singlet and Singlet–Triplet Excitation Energies. *J. Chem. Theory Comput.* **2021**, *17* (8), 5165–5186. <https://doi.org/10.1021/acs.jctc.1c00535>.
- (22) Casanova-Páez, M.; Goerigk, L. Assessing the Tamm–Dancoff Approximation, Singlet–Singlet, and Singlet–Triplet Excitations with the Latest Long-Range Corrected Double-Hybrid Density Functionals. *J. Chem. Phys.* **2020**, *153* (6), 064106.
<https://doi.org/10.1063/5.0018354>.
- (23) Goerigk, L.; Casanova-Paéz, M. The Trip to the Density Functional Theory Zoo Continues: Making a Case for Time-Dependent Double Hybrids for Excited-State Problems. *Aust. J. Chem.* **2021**, *74* (1), 3. <https://doi.org/10.1071/CH20093>.
- (24) Mester, D.; Kállay, M. A Simple Range-Separated Double-Hybrid Density Functional Theory for Excited States. *J. Chem. Theory Comput.* **2021**, *17* (2), 927–942.
<https://doi.org/10.1021/acs.jctc.0c01135>.
- (25) Stoychev, G. L.; Auer, A. A.; Neese, F. Efficient and Accurate Prediction of Nuclear Magnetic Resonance Shielding Tensors with Double-Hybrid Density Functional Theory. *J. Chem. Theory Comput.* **2018**, *14* (9), 4756–4771.
<https://doi.org/10.1021/acs.jctc.8b00624>.
- (26) Tran, V. A.; Neese, F. Double-Hybrid Density Functional Theory for g-Tensor Calculations Using Gauge Including Atomic Orbitals. *J. Chem. Phys.* **2020**, *153* (5), 054105.
<https://doi.org/10.1063/5.0013799>.
- (27) Dittmer, A.; Stoychev, G. L.; Maganas, D.; Auer, A. A.; Neese, F. Computation of NMR Shielding Constants for Solids Using an Embedded Cluster Approach with DFT, Double-Hybrid DFT, and MP2. *J. Chem. Theory Comput.* **2020**, *16* (11), 6950–6967.
<https://doi.org/10.1021/acs.jctc.0c00067>.
- (28) Bursch, M.; Gasevic, T.; Stückrath, J. B.; Grimme, S. Comprehensive Benchmark Study on the Calculation of 29 Si NMR Chemical Shifts. *Inorg. Chem.* **2021**, *60* (1), 272–285.
<https://doi.org/10.1021/acs.inorgchem.0c02907>.

- (29) Alipour, M. How Well Can Parametrized and Parameter-Free Double-Hybrid Approximations Predict Response Properties of Hydrogen-Bonded Systems? Dipole Polarizabilities of Water Nanoclusters as a Working Model. *J. Phys. Chem. A* **2013**, *117* (21), 4506–4513. <https://doi.org/10.1021/jp402659w>.
- (30) Alipour, M. Novel Recipe for Double-Hybrid Density Functional Computations of Linear and Nonlinear Polarizabilities of Molecules and Nanoclusters. *J. Phys. Chem. A* **2014**, *118* (28), 5333–5342. <https://doi.org/10.1021/jp503959w>.
- (31) Grimme, S. Semiempirical Hybrid Density Functional with Perturbative Second-Order Correlation. *J. Chem. Phys.* **2006**, *124* (3), 034108. <https://doi.org/10.1063/1.2148954>.
- (32) Zhang, Y.; Xu, X.; Goddard, W. A. Doubly Hybrid Density Functional for Accurate Descriptions of Nonbond Interactions, Thermochemistry, and Thermochemical Kinetics. *Proc. Natl. Acad. Sci. U. S. A.* **2009**, *106* (13), 4963–4968. <https://doi.org/10.1073/pnas.0901093106>.
- (33) Becke, A. D. Density-functional Thermochemistry. III. The Role of Exact Exchange. *J. Chem. Phys.* **1993**, *98* (7), 5648–5652. <https://doi.org/10.1063/1.464913>.
- (34) Becke, A. D. Density-Functional Exchange-Energy Approximation with Correct Asymptotic Behavior. *Phys. Rev. A* **1988**, *38* (6), 3098–3100. <https://doi.org/10.1103/PhysRevA.38.3098>.
- (35) Stephens, P. J.; Devlin, F. J.; Chabalowski, C. F.; Frisch, M. J. Ab Initio Calculation of Vibrational Absorption and Circular Dichroism Spectra Using Density Functional Force Fields. *J. Phys. Chem.* **1994**, *98* (45), 11623–11627. <https://doi.org/10.1021/j100096a001>.
- (36) Zhang, I. Y.; Xu, X. Reaching a Uniform Accuracy for Complex Molecular Systems: Long-Range-Corrected XYG3 Doubly Hybrid Density Functional. *J. Phys. Chem. Lett.* **2013**, *4* (10), 1669–1675. <https://doi.org/10.1021/jz400695u>.
- (37) Zhang, I. Y.; Xu, X.; Jung, Y.; Goddard, W. A. A Fast Doubly Hybrid Density Functional Method Close to Chemical Accuracy Using a Local Opposite Spin Ansatz. *Proc. Natl. Acad. Sci.* **2011**, *108* (50), 19896–19900. <https://doi.org/10.1073/pnas.1115123108>.
- (38) Kesharwani, M. K.; Kozuch, S.; Martin, J. M. L. Comment on “Doubly Hybrid Density Functional XDH-PBE0 from a Parameter-Free Global Hybrid Model PBE0” [*J. Chem. Phys.* *136*, 174103 (2012)]. *J. Chem. Phys.* **2015**, *143* (18), 187101. <https://doi.org/10.1063/1.4934819>.
- (39) Santra, G.; Cho, M.; Martin, J. M. L. Exploring Avenues beyond Revised DSD Functionals: I. Range Separation, with x DSD as a Special Case. *J. Phys. Chem. A* **2021**, *125* (21), 4614–4627. <https://doi.org/10.1021/acs.jpca.1c01294>.
- (40) Santra, G.; Sylvetsky, N.; Martin, J. M. L. Minimally Empirical Double-Hybrid Functionals Trained against the GMTKN55 Database: RevDSD-PBEP86-D4, RevDOD-PBE-D4, and DOD-SCAN-D4. *J. Phys. Chem. A* **2019**, *123* (24), 5129–5143. <https://doi.org/10.1021/acs.jpca.9b03157>.
- (41) Santra, G.; Semidalas, E.; Martin, J. M. L. Exploring Avenues beyond Revised DSD Functionals: II. Random-Phase Approximation and Scaled MP3 Corrections. *J. Phys. Chem. A* **2021**, *125* (21), 4628–4638. <https://doi.org/10.1021/acs.jpca.1c01295>.
- (42) Mardirossian, N.; Head-Gordon, M. Survival of the Most Transferable at the Top of Jacob’s Ladder: Defining and Testing the ω B97M(2) Double Hybrid Density Functional. *J. Chem. Phys.* **2018**, *148* (24), 241736. <https://doi.org/10.1063/1.5025226>.

- (43) Zhang, I. Y.; Xu, X. Exploring the Limits of the XYG3-Type Doubly Hybrid Approximations for the Main-Group Chemistry: The XDH@B3LYP Model. *J. Phys. Chem. Lett.* **2021**, *12* (10), 2638–2644. <https://doi.org/10.1021/acs.jpcllett.1c00360>.
- (44) Görling, A.; Levy, M. Exact Kohn-Sham Scheme Based on Perturbation Theory. *Phys. Rev. A* **1994**, *50* (1), 196–204. <https://doi.org/10.1103/PhysRevA.50.196>.
- (45) Grimme, S.; Antony, J.; Ehrlich, S.; Krieg, H. A Consistent and Accurate Ab Initio Parametrization of Density Functional Dispersion Correction (DFT-D) for the 94 Elements H-Pu. *J. Chem. Phys.* **2010**, *132* (15), 154104. <https://doi.org/10.1063/1.3382344>.
- (46) Goerigk, L. A Comprehensive Overview of the DFT-D3 London-Dispersion Correction. In *Non-Covalent Interactions in Quantum Chemistry and Physics*; Elsevier, 2017; pp 195–219. <https://doi.org/10.1016/B978-0-12-809835-6.00007-4>.
- (47) Grimme, S.; Ehrlich, S.; Goerigk, L. Effect of the Damping Function in Dispersion Corrected Density Functional Theory. *J. Comput. Chem.* **2011**, *32* (7), 1456–1465. <https://doi.org/10.1002/jcc.21759>.
- (48) Grimme, S.; Bannwarth, C.; Caldeweyher, E.; Pisarek, J.; Hansen, A. A General Intermolecular Force Field Based on Tight-Binding Quantum Chemical Calculations. *J. Chem. Phys.* **2017**, *147* (16), 161708. <https://doi.org/10.1063/1.4991798>.
- (49) Caldeweyher, E.; Ehlert, S.; Hansen, A.; Neugebauer, H.; Spicher, S.; Bannwarth, C.; Grimme, S. A Generally Applicable Atomic-Charge Dependent London Dispersion Correction. *J. Chem. Phys.* **2019**, *150* (15), 154122. <https://doi.org/10.1063/1.5090222>.
- (50) Caldeweyher, E.; Mewes, J.-M.; Ehlert, S.; Grimme, S. Extension and Evaluation of the D4 London-Dispersion Model for Periodic Systems. *Phys. Chem. Chem. Phys.* **2020**, *22* (16), 8499–8512. <https://doi.org/10.1039/D0CP00502A>.
- (51) Kállay, M.; Nagy, P. R.; Mester, D.; Rolik, Z.; Samu, G.; Csontos, J.; Csóka, J.; Szabó, P. B.; Gyevi-Nagy, L.; Hégyel, B.; Ladjánszki, I.; Szegedy, L.; Ladóczki, B.; Petrov, K.; Farkas, M.; Mezei, P. D.; Ganyecz, Á. The MRCC Program System: Accurate Quantum Chemistry from Water to Proteins. *J. Chem. Phys.* **2020**, *152* (7), 074107. <https://doi.org/10.1063/1.5142048>.
- (52) Weigend, F.; Ahlrichs, R. Balanced Basis Sets of Split Valence, Triple Zeta Valence and Quadruple Zeta Valence Quality for H to Rn: Design and Assessment of Accuracy. *Phys. Chem. Chem. Phys.* **2005**, *7* (18), 3297–3305. <https://doi.org/10.1039/b508541a>.
- (53) Rappoport, D.; Furche, F. Property-Optimized Gaussian Basis Sets for Molecular Response Calculations. *J. Chem. Phys.* **2010**, *133* (13), 134105. <https://doi.org/10.1063/1.3484283>.
- (54) Hättig, C. Optimization of Auxiliary Basis Sets for RI-MP2 and RI-CC2 Calculations: Core-Valence and Quintuple-Zeta Basis Sets for H to Ar and QZVPP Basis Sets for Li to Kr. *Phys. Chem. Chem. Phys.* **2005**, *7* (1), 59–66. <https://doi.org/10.1039/b415208e>.
- (55) Weigend, F. Hartree–Fock Exchange Fitting Basis Sets for H to Rn. *J. Comput. Chem.* **2008**, *29* (2), 167–175. <https://doi.org/10.1002/jcc.20702>.
- (56) Frisch, M. J.; Trucks, G. W.; Schlegel, H. B.; Scuseria, G. E.; Robb, M. A.; Cheeseman, J. R.; Scalmani, G.; Barone, V.; Petersson, G. A.; Nakatsuji, H.; Li, X.; Caricato, M.; Marenich, A. V.; Bloino, J.; Janesko, B. G.; Gomperts, R.; Mennucci, B.; Hratchian, H. P.; Ortiz, J. V.; Izmaylov, A. F.; Sonnenberg, J. L.; Williams-Young, D.; Ding, F.; Lipparini, F.; Egidi, F.; Goings, J.; Peng, B.; Petrone, A.; Henderson, T.; Ranasinghe, D.; Zakrzewski, V. G.; Gao, J.;

- Rega, N.; Zheng, G.; Liang, W.; Hada, M.; Ehara, M.; Toyota, K.; Fukuda, R.; Hasegawa, J.; Ishida, M.; Nakajima, T.; Honda, Y.; Kitao, O.; Nakai, H.; Vreven, T.; Throssell, K.; Montgomery Jr., J. A.; Peralta, J. E.; Ogliaro, F.; Bearpark, M. J.; Heyd, J. J.; Brothers, E. N.; Kudin, K. N.; Staroverov, V. N.; Keith, T. A.; Kobayashi, R.; Normand, J.; Raghavachari, K.; Rendell, A. P.; Burant, J. C.; Iyengar, S. S.; Tomasi, J.; Cossi, M.; Millam, J. M.; Klene, M.; Adamo, C.; Cammi, R.; Ochterski, J. W.; Martin, R. L.; Morokuma, K.; Farkas, O.; Foresman, J. B.; Fox, D. J. *Gaussian 16 Revision C.01*; Gaussian, Inc.: Wallingford, CT, 2016.
- (57) Shao, Y.; Gan, Z.; Epifanovsky, E.; Gilbert, A. T. B.; Wormit, M.; Kussmann, J.; Lange, A. W.; Behn, A.; Deng, J.; Feng, X.; Ghosh, D.; Goldey, M.; Horn, P. R.; Jacobson, L. D.; Kaliman, I.; Khaliullin, R. Z.; Kuś, T.; Landau, A.; Liu, J.; Proynov, E. I.; Rhee, Y. M.; Richard, R. M.; Rohrdanz, M. a.; Steele, R. P.; Sundstrom, E. J.; Woodcock, H. L.; Zimmerman, P. M.; Zuev, D.; Albrecht, B.; Alguire, E.; Austin, B.; Beran, G. J. O.; Bernard, Y. a.; Berquist, E.; Brandhorst, K.; Bravaya, K. B.; Brown, S. T.; Casanova, D.; Chang, C.-M.; Chen, Y.; Chien, S. H.; Closser, K. D.; Crittenden, D. L.; Diedenhofen, M.; DiStasio, R. A.; Do, H.; Dutoi, A. D.; Edgar, R. G.; Fatehi, S.; Fusti-Molnar, L.; Ghysels, A.; Golubeva-Zadorozhnaya, A.; Gomes, J.; Hanson-Heine, M. W. D.; Harbach, P. H. P.; Hauser, A. W.; Hohenstein, E. G.; Holden, Z. C.; Jagau, T.-C.; Ji, H.; Kaduk, B.; Khistyayev, K.; Kim, J.; Kim, J.; King, R. a.; Klunzinger, P.; Kosenkov, D.; Kowalczyk, T.; Krauter, C. M.; Lao, K. U.; Laurent, A. D.; Lawler, K. V.; Levchenko, S. V.; Lin, C. Y.; Liu, F.; Livshits, E.; Lochan, R. C.; Luenser, A.; Manohar, P.; Manzer, S. F.; Mao, S.-P.; Mardirossian, N.; Marenich, A. V.; Maurer, S. a.; Mayhall, N. J.; Neuscamman, E.; Oana, C. M.; Olivares-Amaya, R.; O'Neill, D. P.; Parkhill, J. a.; Perrine, T. M.; Peverati, R.; Prociuk, A.; Rehn, D. R.; Rosta, E.; Russ, N. J.; Sharada, S. M.; Sharma, S.; Small, D. W.; Sodt, A.; Stein, T.; Stück, D.; Su, Y.-C.; Thom, A. J. W.; Tsuchimochi, T.; Vanovschi, V.; Vogt, L.; Vydrov, O.; Wang, T.; Watson, M. a.; Wenzel, J.; White, A.; Williams, C. F.; Yang, J.; Yeganeh, S.; Yost, S. R.; You, Z.-Q.; Zhang, I. Y.; Zhang, X.; Zhao, Y.; Brooks, B. R.; Chan, G. K. L.; Chipman, D. M.; Cramer, C. J.; Goddard, W. A.; Gordon, M. S.; Hehre, W. J.; Klamt, A.; Schaefer, H. F.; Schmidt, M. W.; Sherrill, C. D.; Truhlar, D. G.; Warshel, A.; Xu, X.; Aspuru-Guzik, A.; Baer, R.; Bell, A. T.; Besley, N. a.; Chai, J.-D.; Dreuw, A.; Dunietz, B. D.; Furlani, T. R.; Gwaltney, S. R.; Hsu, C.-P.; Jung, Y.; Kong, J.; Lambrecht, D. S.; Liang, W.; Ochsenfeld, C.; Rassolov, V. a.; Slipchenko, L. V.; Subotnik, J. E.; Van Voorhis, T.; Herbert, J. M.; Krylov, A. I.; Gill, P. M. W.; Head-Gordon, M. *Advances in Molecular Quantum Chemistry Contained in the Q-Chem 4 Program Package. Mol. Phys.* **2015**, *113* (2), 184–215. <https://doi.org/10.1080/00268976.2014.952696>.
- (58) Semidalas, E.; Martin, J. M. L. Canonical and DLPNO-Based G4(MP2)XK-Inspired Composite Wave Function Methods Parametrized against Large and Chemically Diverse Training Sets: Are They More Accurate and/or Robust than Double-Hybrid DFT? *J. Chem. Theory Comput.* **2020**, *16* (7), 4238–4255. <https://doi.org/10.1021/acs.jctc.0c00189>.
- (59) Kozuch, S.; Martin, J. M. L. Spin-Component-Scaled Double Hybrids: An Extensive Search for the Best Fifth-Rung Functionals Blending DFT and Perturbation Theory. *J. Comput. Chem.* **2013**, *34* (27), 2327–2344. <https://doi.org/10.1002/jcc.23391>.
- (60) Kozuch, S.; Martin, J. M. L. DSD-PBEP86: In Search of the Best Double-Hybrid DFT with Spin-Component Scaled MP2 and Dispersion Corrections. *Phys. Chem. Chem. Phys.* **2011**,

- 13 (45), 20104. <https://doi.org/10.1039/c1cp22592h>.
- (61) Powell, M. The BOBYQA Algorithm for Bound Constrained Optimization without Derivatives (DAMPT Report 2009/NA06); Department of Applied Mathematics and Theoretical Physics, University of Cambridge, UK, 2009.
- (62) Schwarz, G. Estimating the Dimension of a Model. *Ann. Stat.* **1978**, *6* (2), 461–464. <https://doi.org/10.1214/aos/1176344136>.
- (63) Kass, R. E.; Raftery, A. E. Bayes Factors. *J. Am. Stat. Assoc.* **1995**, *90* (430), 773–795. <https://doi.org/10.1080/01621459.1995.10476572>.
- (64) Grimme, S. Improved Third-Order Møller-Plesset Perturbation Theory. *J. Comput. Chem.* **2003**, *24* (13), 1529–1537. <https://doi.org/10.1002/jcc.10320>.
- (65) Pitoňák, M.; Neogrady, P.; Černý, J.; Grimme, S.; Hobza, P. Scaled MP3 Non-Covalent Interaction Energies Agree Closely with Accurate CCSD(T) Benchmark Data. *ChemPhysChem* **2009**, *10* (1), 282–289. <https://doi.org/10.1002/cphc.200800718>.
- (66) Rettig, A.; Hait, D.; Bertels, L. W.; Head-Gordon, M. Third-Order Møller–Plesset Theory Made More Useful? The Role of Density Functional Theory Orbitals. *J. Chem. Theory Comput.* **2020**, *16* (12), 7473–7489. <https://doi.org/10.1021/acs.jctc.0c00986>.
- (67) Lee, J.; Lin, L.; Head-Gordon, M. Systematically Improvable Tensor Hypercontraction: Interpolative Separable Density-Fitting for Molecules Applied to Exact Exchange, Second- and Third-Order Møller–Plesset Perturbation Theory. *J. Chem. Theory Comput.* **2020**, *16* (1), 243–263. <https://doi.org/10.1021/acs.jctc.9b00820>.
- (68) Jana, S.; Śmiga, S.; Constantin, L. A.; Samal, P. Generalizing Double-Hybrid Density Functionals: Impact of Higher-Order Perturbation Terms. *J. Chem. Theory Comput.* **2020**, *16* (12), 7413–7430. <https://doi.org/10.1021/acs.jctc.0c00823>.
- (69) Semidalas, E.; Martin, J. M. L. Canonical and DLPNO-Based Composite Wavefunction Methods Parametrized against Large and Chemically Diverse Training Sets. 2: Correlation-Consistent Basis Sets, Core–Valence Correlation, and F12 Alternatives. *J. Chem. Theory Comput.* **2020**, *16* (12), 7507–7524. <https://doi.org/10.1021/acs.jctc.0c01106>.
- (70) Matthews, D. A. A Critical Analysis of Least-Squares Tensor Hypercontraction Applied to MP3. *J. Chem. Phys.* **2021**, *154* (13), 134102. <https://doi.org/10.1063/5.0038764>.
- (71) Hohenstein, E. G.; Parrish, R. M.; Martínez, T. J. Tensor Hypercontraction Density Fitting. I. Quartic Scaling Second- and Third-Order Møller-Plesset Perturbation Theory. *J. Chem. Phys.* **2012**, *137* (4), 1085. <https://doi.org/10.1063/1.4732310>.

TOC graphic (scalable):

